CSIRO PUBLISHING

Functional Plant Biology, 2015, **42**, 858–864
http://dx.doi.org/10.1071/FP15024

High resolution imaging of maize (*Zea mays*) leaf temperature in the field: the key role of the regions of interest

Taha Jerbi[A], *Nathalie Wuyts*[A,B], *Maria Angela Cane*[C], *Philippe-François Faux*[A] *and Xavier Draye*[A,D]

[A]Earth and Life Institute, Université catholique de Louvain, Croix du Sud 2 L7.05.11, 1348 Louvain-la-Neuve, Belgium.
[B]Present address: Department of Plant Systems Biology, Vlaams Instituut voor Biotechnologie, Technologie Park, 9000 Gent, Belgium.
[C]Di.S.T.A. Department of Agroenvironmental Sciences and Technologies, University of Bologna, Viale Fanin 44, 40127 Bologna, Italy.
[D]Corresponding author. Email: xavier.draye@uclouvain.be

Abstract. The use of remote sensors (thermometers and cameras) to analyse crop water status in field conditions is fraught with several difficulties. In particular, average canopy temperature measurements are affected by the mixture of soil and green regions, the mutual shading of leaves and the variability of absorbed radiation. The aim of the study was to analyse how the selection of different 'regions of interest' (ROI) in canopy images affect the variability of the resulting temperature averages. Using automated image segmentation techniques we computed the average temperature in four nested ROI of decreasing size, from the whole image down to the sunlit fraction of a leaf located in the upper part of the canopy. The study was conducted on maize (*Zea mays* L.) at the flowering stage, for its large leaves and well structured canopy. Our results suggest that, under these conditions, the ROI comprising the sunlit fraction of a leaf located in the upper part of the canopy should be analogous to the single leaf approach (in controlled conditions) that allows the estimation of stomatal conductance or plant water potential.

Additional keywords: canopy, phenotyping, remote sensing, segmentation, thermography.

Received 22 February 2014, accepted 7 May 2015, published online 15 June 2015

Introduction

Monitoring crop water status at critical phenological stages is an important task for irrigation scheduling, and allows for the identification of genotypes that are able to maintain transpiration under water deficit, as well as for analysing mechanisms underlying drought tolerance (Costa *et al*. 2013). Canopy temperature is used operationally to compute various water stress indices (reviewed by Maes and Steppe 2012), as it is easily obtained by remote sensing and relates to plant transpiration through the cooling effect of evaporation at the leaf surface.

Physical relations relating leaf temperature to stomatal conductance and leaf water potential in controlled conditions have been established and validated experimentally (Jones 1999*b*; Cohen *et al*. 2005). However, the use of remotely-sensed temperatures to quantify plant water status in the field is fraught with several difficulties, primarily because environmental conditions influence the heat balance and temperature of leaves. Several normalisation techniques have been proposed to remove the effect of these environmental influences from sensed values. These techniques rely on air temperature (Jackson *et al*. 1977), non-transpiring and non-stressed crop temperatures (Idso *et al*. 1981), physical reference surface temperatures (Jones 1999*a*) and, more recently, theoretical wet and dry reference temperatures (Leinonen *et al*. 2006).

Scaling up remote sensing techniques from individual leaves to crop canopies also introduces issues related to the complexity of the canopy within the field of view of the sensor (Jones *et al*. 2009). When using thermometer sensors or thermal cameras with low spatial resolution compared with the leaf size, the measurements provide an average value over a collection of objects. That value can be used to estimate various indices of crop water status, as long as one is confident that the sensor is recording the temperature of the leaves of interest (Grant *et al*. 2007; Zia *et al*. 2013). More sophisticated approaches are possible with ground-based remote sensing using high resolution thermal and visible (RGB) cameras. In these conditions, the segmentation of the RGB image provides a mask of leaves that is applied on the thermal image to obtain a temperature measurement of the green area of the canopy ignoring background temperature (Leinonen and Jones 2004).

Temperature variations up to 10–15°C occur among leaves of a canopy as well as along individual leaves (Jones *et al*. 2002;

Grant *et al*. 2007; see Fig. 1). Consequently, the green mask that is obtained by the segmentation of RGB image still contains a population of leaf segments with contrasting age, exposition and environmental conditions, depending on their position in the canopy and on the direction of solar radiation. This variability has been exploited with a variable success to estimate stomatal conductance, based on the rationale that transpiration smoothes the temperature variation between leaves of the canopy (Fuchs 1990; see review by Jones *et al*. 2009).

The variability of leaf temperature in a canopy has been attributed mainly to the effect of absorbed radiation, resulting from mutual shading, position in the canopy and the major effect of leaf angle (Jones *et al*. 2009). Prior investigations of the influence of the leaf orientation suggested that the mean canopy temperature is a less variable measurement than leaf temperature, due to the implicit averaging of the leaf angle (Grant *et al*. 2007). However, such averaging is likely to introduce confounding effects for at least two reasons. First, the information content of individual leaf segments with respect to the derivation of physiological crop parameters varies among segments; and second, their absorbed radiation cannot be considered as random as it depends on canopy architecture and on the direction of solar radiation.

Our study takes advantage of image segmentation techniques to perform the automated selection of four nested 'regions of interest' (ROI) of decreasing size, from the whole image down to the sunlit fraction of a leaf located in the upper part of the canopy. The aim of the study was to compare the variability of temperature measurements averaged within these regions. Maize (*Zea mays* L.) canopies at the flowering stage were chosen for this analysis. Given the large leaves of this species, image segmentation yields areas comprised of hundred of pixels and it can be assumed that the averaging is not affected by sample size issues. In addition, the maize canopy is structured in a way such that leaves in the row are most likely to be upper leaves, and leaves between rows are located at an intermediate height. Our results suggest that, in these conditions, the ROI comprising the sunlit fraction of a leaf located in the upper part of the canopy should be analogous to the single leaf approach in controlled conditions that allows the estimation of stomatal conductance or plant water potential.

Materials and methods

Image data

For this analysis, we selected 74 images of maize canopies from the image database of the DROPs project (www.drops-project.eu, accessed 22 May 2015). This database contained thousands of images acquired in 2011 and 2012 during the flowering period of maize in large scale field trials (250 hybrids) located in Bologna (Italy). Images had been acquired using a thermal camera (FLIR SC660 http://www.flir.eu/science/content/?id=41965, accessed 22 May 2015) mounted on a pole, ~1 m above the top of the canopy, with a vertical orientation of the field of view. The camera provides thermal and visible (RGB) modalities, with sensor sizes of 480 ×640 and 1536 ×2048 respectively.

The selection of images for our analysis aimed at assembling a set of images embracing a range of canopy structure, leaf exposition, solar radiation and plant water status. For this purpose, images were picked from a subset of six hybrids with different canopy structures (W64A, F894, PH207, B73, Oh-43, MS153, all crossed to UH007 as tester). The selected set of images also embraces different hours and days of acquisition, viz. between 0800 and 1700 hours within a period of seven consecutive days during which the field was not irrigated (drying cycle).

General scheme of the algorithm

A general pipeline was set up using Microsoft Visual C^{++} and the open-source library ITK to compute the average temperature in different ROI (Fig. 2). A registration was first carried out to establish pixel-to-pixel correspondence between IR and RGB modalities. Images were then segmented to mark different ROI, namely (i) the whole image, (ii) the whole canopy (after exclusion of the soil pixels), (iii) a large leaf aligned on the field row, and (iv) the sunlit part of that leaf. The average temperature was then calculated in the four ROI for each of the 74 images. The different imaging steps are described hereafter.

Registration

A registration was required to establish the pixel-to-pixel correspondence between the IR and RGB modalities produced

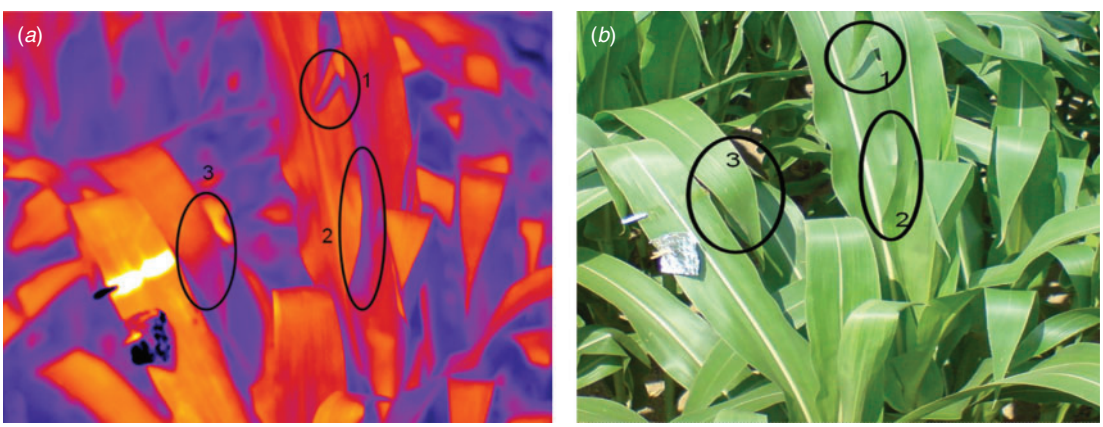

Fig. 1. High resolution infrared (*a*) and RGB (*b*) images of a maize canopy. Circles 1 to 3 illustrate the effect of, respectively, mutual shading, leaf rolling and orientation on the spatial variation of temperature along leaves.

by different imaging sensors (Fig. 3 top row). This requires a transformation to match the images and a similarity criterion to measure the difference between the images. In a similar work (Yang *et al*. 2009), the transformation between the images used a translation, a rotation and a scale factor. We used the same kind of transformation as the risk of non-rigid motion of leaves during the small delay between RGB and IR acquisition had been reduced by selecting images acquired in the absence of wind.

The differences between images was quantified with a distance based on the normalised correlation metric, which was previously identified as the best measure for multi-modal registration in medical applications (Penney *et al*. 1998). Yang *et al*. (2012) applied a normalised cross correlation (NCC) metric on the gradient (by using a modified Sobel edge detector to get the contours) and a multiscale registration scheme to get a first rough registration. Their approach is justified where regions with higher intensity in one image have lower intensity in the other. In our case, the NCC metric was applied directly to the pixels grey level intensity (Penney *et al*. 1998).

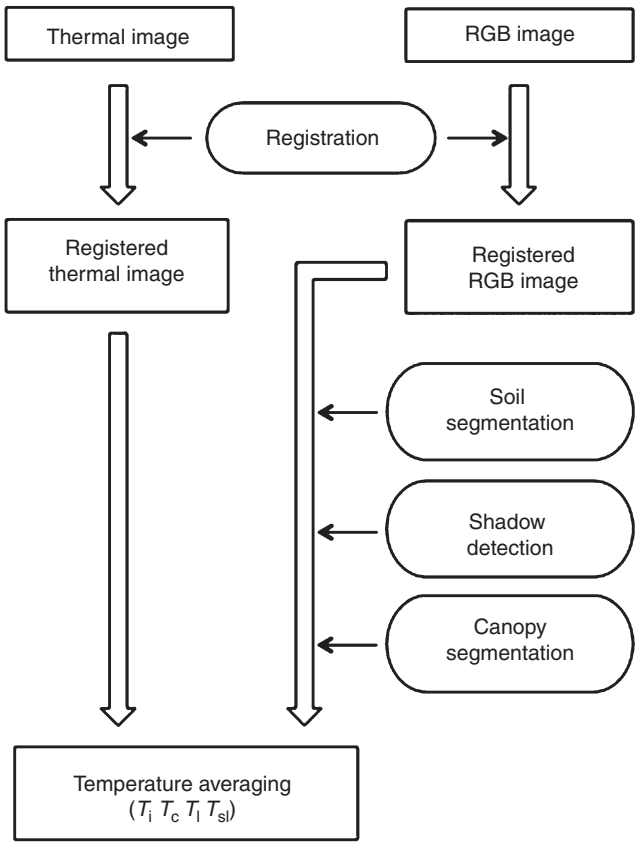

Fig. 2. Workflow of the automated image processing pipeline.

Acquisitions of a chessboard pattern were used to validate the registration method. The chessboard was printed on a white paper which was placed on window in a sunny day in order to obtain a temperature difference between the white and black squares. The registration errors for these tests were evaluated by measuring the difference between the positions of the corners in the two images. These errors were less than two pixels. Fig. 3 illustrates the results obtained by registering visible and infrared images of a maize canopy.

Soil detection

A segmentation procedure was used to split thermal images into uniform regions with the aim to separate soil pixels from canopy pixels. As the separation between objects was not always clear in the infrared modality, the segmentation was done using the RGB modality. It was achieved using a watershed algorithm that separates regions of the image using an analogy with the flooding of a natural relief. Where the water in two different basins merges, a line separating two different regions of the image is formed. In the image segmentation case, the relief corresponded to the gradient of the image. This algorithm is one of the most popular in the image segmentation field (Bieniek and Moga 2000). The threshold gradient value separating neighbour regions was set empirically in order to reduce the risk of over-segmentation (the major drawback of the watershed algorithm). A unique value was found to be suitable for the complete set of images, despite the varying levels of light levels and quality across images. This was essentially due to the steep gradient appearing at the boundaries between soil and canopy pixels. Finally, the labelling of every region into soil or canopy classes could be made according to their average RGB profile.

Shadow detection

Detecting the shaded areas of the canopy was a preliminary step to compute the average temperature of the sunlit canopy fraction.

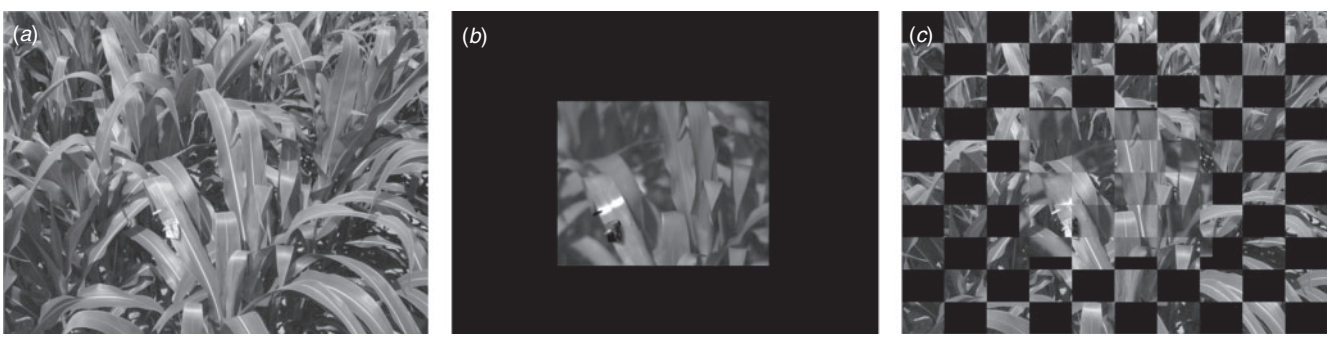

Fig. 3. Illustration of the registration process. RGB (*a*) and thermal (*b*) images. The black frame around the thermal image indicates the field of view of the RGB image. (*c*) A chess-like composite overlay of the RGB and thermal images after registration that illustrates the quality of the registration. The rectangle at position *i*, *j* (i, j ∈ [1, 10]) shows the corresponding area of the RGB modality if (*i*+*j*) is odd and of the thermal modality if (*i*+*j*) is even.

The RGB images were transformed to the HSV (hue, saturation, value) colour system and a normalised saturation-value difference index was computed for each pixel (Ma *et al*. 2008). The separation of shaded and sunny leaf pixels was then made by conventional thresholding (Ma *et al*. 2008). This method was tested on several canopy images and was compared with a manual tracing of shadowed areas. The comparison revealed that the proportion of mis-classified pixels (in the 'shadowed' class in one method and in the 'sunny' class in the other) was less than 2%. It was ~1.59% on the image illustrated in Fig. 4. The manual selection of the shadow area took to the expert nearly half an hour whereas this method provided results in just few seconds.

Leaf selection

Using the results of the segmentation above, a single leaf located in the centre of the image and with a large area was selected as a representative leaf. This ensured (i) that the selected leaf belonged to a plant located in the central row and not to a plant from a neighbouring row (with a different genotype), and (ii) that the representative leaf was located in the top part of the canopy, with a minimum shadowed area.

Finally, the shadowed area of the image was subtracted from the area of the single leaf to obtain a mask of the sunlit fraction of that leaf. We assumed that this leaf fraction should be in exposure conditions similar to the single leaf approach by Jones (1999*b*).

Temperature averaging

Using the results of the registration, the various ROI obtained in the RGB modality were used to compute average temperatures in the corresponding areas of the thermal modality. Four temperature estimates were obtained in this way: (i) the average temperature of the whole image (T_i), (ii) the average temperature of the whole canopy (i.e. after exclusion of the soil pixels) (T_c), (iii) the average temperature of the representative leaf (T_l), and (iv) the average temperature of the sunlit part of the representative leaf (T_{sl}).

Finally, we compared the different estimates over the sample of 74 images which represented a wide range of conditions for maize at flowering. Small differences could have arisen during image processing (segmentation, registration) and should not be considered as meaningful. We considered a conservative baseline of 1.5°C, which is below genotypic differences of leaf temperature of 1.8–3.7°C reported under field conditions (Jones *et al*. 2009).

Results

Fig. 5 reports the range of the four temperature estimates for each of the 74 images. As expected, there was a large effect of the time of day, with a ~6°C difference between 0900 and 1200 hours, which resulted presumably from differences in absorbed radiation and plant transpiration (Jones *et al*. 2009). Although not directly visible on the figure, there were also differences up to 7°C between images for the same ROI. These most likely resulted from a mixture of the effects of canopy structure (hybrid) and plant water status (day during the drying cycle).

In this set of data, only small differences were found between the temperature of the canopy (T_c) and the temperature of the whole image (T_i) ($r > 0.99$, Fig. 6*a*). This has to be related to the fact that acquisitions had been done near flowering, when plants have reached their maximal leaf area. In these conditions, the soil is largely under the shadow of the plants and soil areas in the field of view of the camera tend to be small. The largest soil region comprised 51 615 pixels (16% of the image pixel count) and the corresponding temperature difference $|T_i - T_c|$ was only 0.46°C.

To further assess the effect of soil pixels on T_i, we analysed 12 acquisitions (not comprised in the 74) in which sunlit soil pixels comprised 25–96% of the image (Fig. 7). Because sunlit soil pixels tend to have larger temperatures than leaves, the difference ($T_i - T_c$) increased with increasing fraction of soil pixels. ($T_i - T_c$) reached 2°C with a soil fraction of 25–40%, 5°C with a soil fraction of 40–85%, 10°C with 85% and up to 12.7°C for a soil fraction of 96%. As the structure of the canopy itself determines the size of the soil area (in acquisitions made from the top of the canopy), average image temperatures carry a genotype dependent bias that could affect their assessment.

On the majority of images, the temperature of the representative leaf (T_l) and that of the sunlit part of that leaf (T_{sl}) were higher than T_i (Fig. 6*b*, *c*) and T_c, a consequence of the

Fig. 4. Illustration of the shadow detection process. The left image is the original RGB. The right image is the processed image after masking pixels corresponding to shadow areas.

selected leaf being in the top of the canopy and of the heating effect of radiation absorption in sunlit parts. The correlation between T_i and T_l was 0.95 and that between T_i and T_{sl} was 0.93. T_l and T_{sl} exceeded T_i by, respectively, 0.7 and 1.2°C on average, or by 1.5°C in, respectively, 19 and 32% of the images. T_l and T_{sl} were also highly correlated (Fig. 6*d*) and displayed an average difference of 0.5°C.

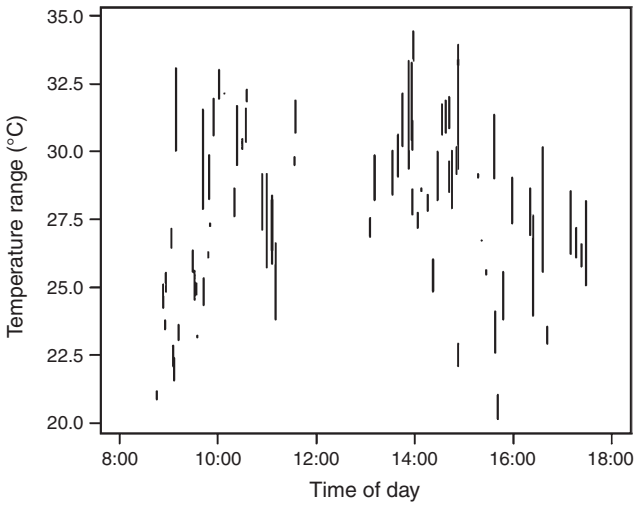

Fig. 5. Dependence of leaf temperature on the time of day. Each bar corresponds to a single image and represents the range (min–max) of temperatures estimated from the image using the four regions of interest.

An examination of metadata indicated that images with low ($T_l - T_i$) or ($T_{sl} - T_i$) differences had been acquired early in the morning, i.e. under diffuse day light and limited solar radiation. This is not surprising as, compared with mid-day acquisitions, the absorption of radiation by the top and exposed leaves was reduced in the early morning and the temperature contrast between the two tended to be smaller.

The set of ROI considered here constitutes a nested series of regions of increasing complexity and area {well exposed leaf area} ⊂ {representative leaf} ⊂ {whole canopy} ⊂ {whole image}. To estimate the benefit of the shadow exclusion and of the segmentation of a single leaf, we estimated the variance (across the 74 images) of the four temperature indicators. The variance of T_{sl} (11.01) turned out to be 22% larger than that of T_l (9.18), T_c (9.13) and T_i (9.09). This result indicates that the inclusion of shaded leaf parts and soil inside the ROI did not increase the variance across images but, on the contrary, seemed to smooth out the differences of the sunlit parts. This suggests that the temperature of the shaded or bottom part of the canopy tends to be more stable across scenes than that of the sunlit canopy fraction.

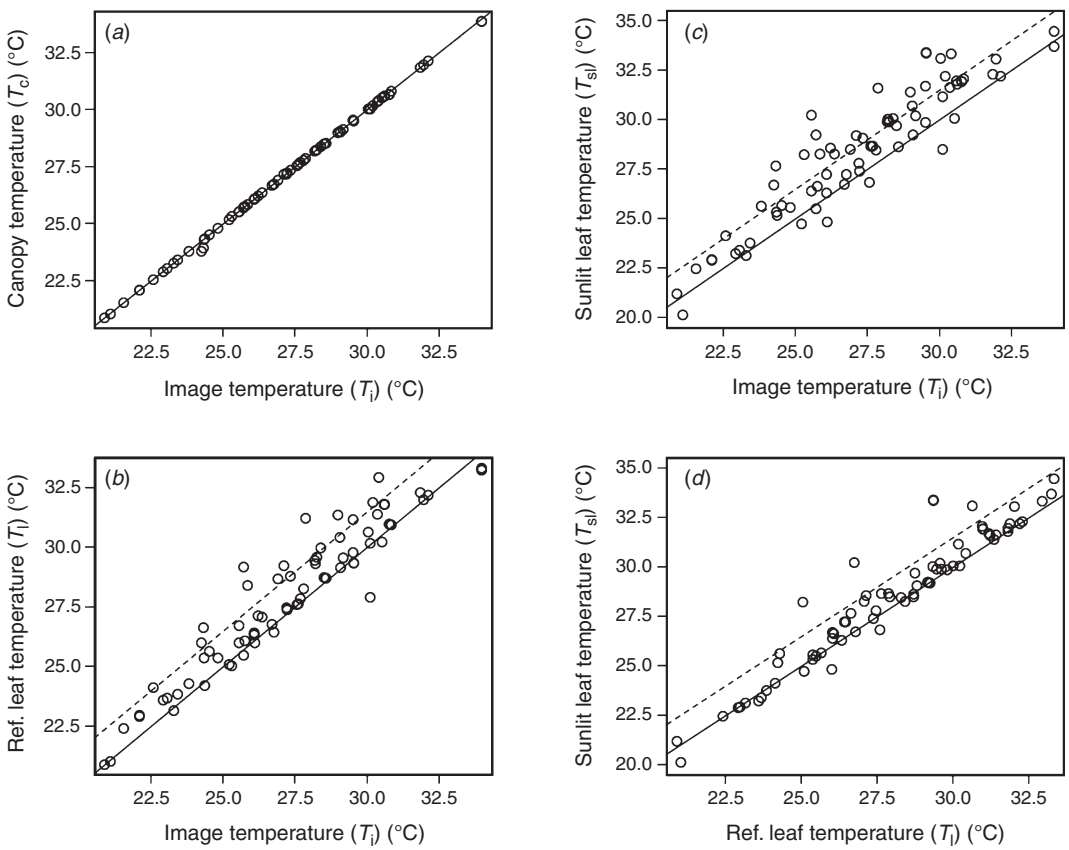

Fig. 6. Relationships between the temperature estimates of the different regions of interest. Each point represents one of the 74 images. Plain lines indicate the 1 : 1 relationship. Dotted lines indicate a +1.5°C shift of the ordinate relative to the 1 : 1 relationship.

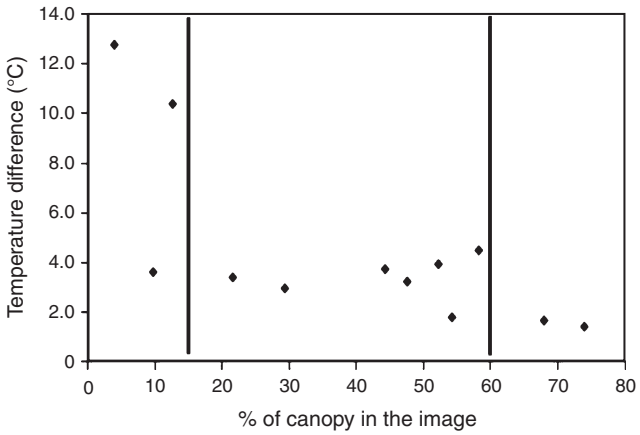

Fig. 7. Illustration of the difference between image and canopy temperature ($T_i - T_c$) as a function of the canopy fraction (percentage of canopy pixels in the image). Results obtained with an additional set of 12 images providing a large amplitude of canopy fraction.

Discussion

In this study, we propose an automated image analysis pipeline combining high resolution IR and RGB image modalities to estimate the leaf temperature of maize plants in the field during the flowering period. The pipeline includes the registration of the IR and RGB modalities and uses segmentation algorithms to estimate the temperature of four ROIs of decreasing complexity, from the whole image to the sunlit fraction of a single leaf. This pipeline is then used on a set of contrasting scenes (different genotypes, time-of-day and level of water deficit) to study the major benefits of high resolution thermal imaging in field conditions, in comparison with intermediate or low resolution imaging techniques.

It has been recently reported that the average temperature of the green area of maize rows can be used to differentiate maize hybrids of contrasting phenologies in field conditions (Zia *et al*. 2013). Our results strengthen the grounds of this statement by showing that the average canopy temperature correlates with the temperature of the sunlit canopy fraction, for which the physiological basis of leaf temperature has been established (Jones *et al*. 2009). However, the observation that the inclusion of shaded leaf parts and soil smoothed out the differences between scenes indicates that the selection of a single well-exposed leaf area has the potential to reveal differences among scenes that would be filtered out without segmentation. We note that these differences might be significant for field phenotyping, as scene and leaf temperatures differed by a value that can be greater than genotypic differences reported elsewhere (Liu *et al*. 2011), especially under direct solar radiation. Therefore, we propose that the use of the temperature of the sunlit canopy fraction has the potential to improve the reliability of thermal imaging for field phenotyping applications (Leinonen *et al*. 2006). However, the experimental validation of this proposition requires the demonstration that the information carried by the higher temperature variation of the sunlit canopy fraction, compared with that of the rest of the canopy, is actually relevant for a physiological interpretation.

In the method we applied to maize, we pushed further this 'leave of interest' problem and evaluated the relevance of extracting a unique leaf aligned on the planting row. Given the structure of the maize canopy, the selection of a leaf aligned on the row narrows the age range of the leaves analysed across different images and reduces the age-related variability in stomatal conductance and leaf temperature. The selected leaf ROI may therefore be a better choice to reveal differences between genotypes compared with the use of larger ROIs. In addition, since the corresponding leaf is located in the upper part of the canopy, meteorological data obtained with on-site stations provide an accurate description of its local environment. The obtained results are ultimately analogous to the single leaf approach for which the accuracy of thermal imaging has been established (Maes and Steppe 2012). A possible improvement of the method would be to take into account the orientation of the leaf segment relative to the sun, which would provide a better estimate of the specific radiation absorption by the selected leaf. With the large area of maize leaves, this spatial information might be captured by time-of-flight cameras or LiDar equipment.

The extraction of temperature of the leaves of interest from whole canopy images has been highlighted as a major problem in the scaling up of thermal imaging from leaves in controlled conditions to real canopies (Jones *et al*. 2009). The notion of 'leaves of interest' reflects different realities depending on the chosen estimation method. In the study by Wang *et al*. (2010), for example, the problem was to identify wet and dry reference leaves, based on their relative position to a reference object or on their temperature ranking. When reference temperatures are known (Leinonen *et al*. 2006), the focus moved to the selection of a part of the canopy that carries the most relevant information. The elimination of the shadowed canopy fraction has been proposed as an appropriate filtering strategy (Leinonen and Jones 2004). It is based on the premise that the sunlit parts of the canopy are generally comprised of the young leaves with highest hydraulic conductance, are the most distant from the roots, and are exposed to the driest atmospheric conditions and to the highest solar radiation. Sunlit leaves are therefore likely to be a rather sensitive sensor of plant water status (Leinonen and Jones 2004; Möller *et al*. 2007). However, shadow exclusion is not generally applied, seemingly because of difficulties for its implementation (Prashar *et al*. 2013). The algorithm that we have developed appears to be generally applicable to canopies of adult maize plants, characterised by long and large leaves that ease segmentation.

Unlike intermediate resolution techniques (e.g. Zia *et al*. 2013), high resolution imaging enables the exclusion of soil and shaded leaves or the segmentation of a sunlit leaf fraction and the use of automated segmentation algorithms to dramatically improve the throughput of image analysis downstream of acquisition. However, the high spatial resolution is only compatible with 640×480 cameras maintained ~1 m above the canopy, which prevents achieving the throughput requirement of phenotyping applications. It is expected that the decreasing costs and miniaturisation of thermal sensors will make it realistic to embark thermal cameras on board small UAVs (Maes and Steppe 2012), which will provide the needed flexibility for scene acquisition at the field scale when atmospheric conditions are suitable.

Acknowledgements

This work was supported by the European Community's Seventh Framework Program under the grant agreement n°FP7–244374 (DROPs) (TJ, MAC, XD), by the Fonds Spéciaux de Recherche from the Université catholique de Louvain (TJ) and by the Fonds de la Recherche Fondamentale Collective (FRFC, grant n°2.4537.10) (NW).

References

Bieniek A, Moga A (2000) An efficient watershed algorithm based on connected components. *Pattern Recognition* **33**, 907–916. doi:10.1016/S0031-3203(99)00154-5

Cohen Y, Alchantis V, Meron M, Saranga Y, Tsipris J (2005) Estimation of leaf water potential by thermal imagery and spatial analysis. *Journal of Experimental Botany* **56**, 1843–1852. doi:10.1093/jxb/eri174

Costa JM, Grant OM, Chaves MM (2013) Thermography to explore plant–environment interactions. *Journal of Experimental Botany* **64**, 3937–3949. doi:10.1093/jxb/ert029

Fuchs M (1990) Infrared measurement of canopy temperature and detection of plant water stress. *Theoretical and Applied Climatology* **42**, 253–261. doi:10.1007/BF00865986

Grant OM, Tronina L, Jones HG, Chaves MM (2007) Exploring thermal imaging variables for the detection of stress responses in grapevine under different irrigation regimes. *Journal of Experimental Botany* **58**, 815–825. doi:10.1093/jxb/erl153

Idso S, Jackson R, Pinter P, Reginato R, Hateld J (1981) Normalizing the stress degree day parameter for environmental variability. *Agricultural Meteorology* **24**, 45–55. doi:10.1016/0002-1571(81)90032-7

Jackson RD, Reginato RJ, Idso SB (1977) Wheat canopy temperature: a practical tool for evaluating water requirements. *Water Resources Research* **13**, 651–656. doi:10.1029/WR013i003p00651

Jones HG (1999*a*) Use of infrared thermometry for estimation of stomatal conductance as a possible aid to irrigation scheduling. *Agricultural and Forest Meteorology* **95**, 139–149. doi:10.1016/S0168-1923(99)00030-1

Jones HG (1999*b*) Use of thermography for quantitative studies of spatial and temporal variation of stomatal conductance over leaf surfaces. *Plant, Cell & Environment* **22**, 1043–1055. doi:10.1046/j.1365-3040.1999.00468.x

Jones HG, Stoll M, Santos T, de Sousa C, Chaves MM, Grant OM (2002) Use of infrared thermography for monitoring stomatal closure in the field: application to grapevine. *Journal of Experimental Botany* **53**, 2249–2260. doi:10.1093/jxb/erf083

Jones HG, Serraj R, Loveys BR, Xiong L, Wheaton A, Price AH (2009) Thermal infrared imaging of crop canopies for the remote diagnosis and quantification of plant responses to water stress in the field. *Functional Plant Biology* **36**, 978–989. doi:10.1071/FP09123

Leinonen I, Jones HG (2004) Combining thermal and visible imagery for estimating canopy temperature and identifying plant stress. *Journal of Experimental Botany* **55**, 1423–1431. doi:10.1093/jxb/erh146

Leinonen I, Grant OM, Tagliavia CPP, Chaves MM, Jones HG (2006) Estimating stomatal conductance with thermal imagery. *Plant, Cell & Environment* **29**, 1508–1518. doi:10.1111/j.1365-3040.2006.01528.x

Liu Y, Subhash C, Yan J, Song C, Zhao J, Li J (2011) Maize leaf temperature responses to drought: Thermal imaging and quantitative trait loci (QTL) mapping. *Environmental and Experimental Botany* **71**, 158–165. doi:10.1016/j.envexpbot.2010.11.010

Ma H, Qin Q, Shen X (2008) Shadow segmentation and compensation in high resolution satellite images. Geoscience and remote sensing symposium. In 'Geoscience and Remote Sensing Symposium'. (IEEE International: New York)

Maes WH, Steppe K (2012) Estimating evapotranspiration and drought stress with ground-based thermal remote sensing in agriculture: a review. *Journal of Experimental Botany* **63**, 4671–4712. doi:10.1093/jxb/ers165

Möller M, Alcanatis V, Cohen Y, Meron M, Tsipris J, Naor A, Ostrovsky V, Sprintsin M, Cohen S (2007) Use of thermal and visible imagery for estimating crop water status of irrigated grapevine. *Journal of Experimental Botany* **58**, 827–838. doi:10.1093/jxb/erl115

Penney G, Weese J, Little J, Desmedt P, Hill D, Hawkes D (1998) 290 A comparison of similarity measures for use in 2D–3D medical image registration. *IEEE Transactions on Medical Imaging* **17**, 586–595. doi:10.1109/42.730403

Prashar A, Yildiz J, McNicol J, Bryan G, Jones HG (2013) Infrared thermography for high throughput field phenotyping in *Solanum tuberosum*. *PLoS One* **8**, e65816. doi:10.1371/journal.pone.0065816

Wang X, Yang W, Wheaton A, Cooley N, Morana B (2010) Automated canopy temperature estimation via infrared thermography: a first step towards automated plant water stress monitoring. *Computers and Electronics in Agriculture* **73**, 74–83. doi:10.1016/j.compag.2010.04.007

Yang W, Wang X, Wheaton A, Cooley N, Moran B (2009) Automatic optical and IR image fusion for plant water stress analysis. In '12th International Conference on Information Fusion'. pp. 1053–1059. (IEEE International: New York)

Yang W, Wang X, Moran B, Wheaton A, Cooley N (2012) Efficient registration of optical and infrared images via modified Sobel edging for plant canopy temperature estimation. *Computers & Electrical Engineering* **38**, 1213–1221. doi:10.1016/j.compeleceng.2012.05.014

Zia S, Romano G, Spreer W, Sanchez C, Cairns J, Araus JL, Müller J (2013) Infrared thermal imaging as a rapid tool for identifying water-stress tolerant maize genotypes of different phenology. *Journal Agronomy & Crop Science* **199**, 75–84. doi:10.1111/j.1439-037X.2012.00537.x